

International Journal of Pharmacology

ISSN 1811-7775





ISSN 1811-7775 DOI: 10.3923/ijp.2024.1488.1500



Research Article

Mechanism of *Ganoderma lucidum* Polysaccharides Mediating NF-κB Signaling Pathway-Related Proteins Alleviating Post-Anesthesia Inflammation in Retinal Cells

Na Li

Operating Room, West China Hospital, Sichuan University/West China School of Nursing, Sichuan University, Chengdu 610041, Sichuan, China

Abstract

Background and Objective: Post-anesthesia inflammation in retinal cells is a remarkable ocular complication that could lead to vision issues. This study was aimed to investigate the mechanism of action of *Ganoderma lucidum* polysaccharides (GIP), a naturally derived extract, on the inflammatory response of retinal cells. Materials and Methods: The GIPs were extracted and the total sugar content was determined by the phenol-sulfuric acid method, with reducing sugar content assessed using the DNS method. In vivo experiments, 50 Sprague-Dawley rats were selected to establish a model of post-anesthesia retinal cell inflammation and were divided into control, model and three GIP treatment groups (treated with 50, 100 and 150 mg/kg of GIP, respectively). Comparative analyses included retinal electrophysiological examinations, retinal thickness measurements and evaluation of inflammatory factors. In vitro experiments, retinal cells were cultured to analyze the expression level (EL) of Bcl-2, Bax and Caspase-3 in various groups. The PCR analysis was performed to determine the relative mRNA ELs of NF-κB, LOX-1, TRAF-6 and TLR-4 in the various groups. Results: The cold-water immersion method yielded consistent GIP extraction rates around 39%, with negligible differences (p>0.05). In vivo, GIP treatment significantly increased a-wave and b-wave amplitudes in retinal electrophysiology compared to the model group, showing dose dependency (p<0.05). The GIP administration also decreased inflammatory factors (VEGF, TNF- α , IL-1 β , IL-6, ICAM-1 and IL-1 β) in rat serum and inhibited retinal cell apoptosis. *In vitro*, GIP treatment reduced mRNA expression levels of NF-κB, TLR-4 and TRAF-6, indicating its potential to mitigate inflammation and promote cell survival (p<0.05). **Conclusion:** The cold-water immersion methodology is effective in extracting GIPs with repeatability and reliability. The natural extract of GIPs dramatically inhibits the inflammation of post-anesthesia retinal cells, potentially involving the modulation of the NF-kB signaling.

Key words: Ganoderma lucidum polysaccharides, NF-κB signaling, ophthalmic anesthesia, retinal cells, inflammatory response

Citation: Li, N., 2024. Mechanism of $Ganoderma\ lucidum\$ polysaccharides mediating NF- κB signaling pathway-related proteins alleviating post-anesthesia inflammation in retinal cells. Int. J. Pharmacol., 20: 1488-1500.

Corresponding Author: Na Li, Operating Room, West China Hospital, Sichuan University/West China School of Nursing, Sichuan University, Chengdu 610041, Sichuan, China

Copyright: © 2024 Na Li. This is an open access article distributed under the terms of the creative commons attribution License, which permits unrestricted use, distribution and reproduction in any medium, provided the original author and source are credited.

Competing Interest: The author has declared that no competing interest exists.

Data Availability: All relevant data are within the paper and its supporting information files.

INTRODUCTION

Anesthesia in ophthalmic surgeries is a common clinical practice. However, complications associated with it, especially post-anesthesia inflammation in retinal cells, have remained a focal point of concern for clinicians and researchers. This type of inflammation can lead to vision problems and in severe cases, it might even pose a threat to the survival of retinal cells. Hence, investigating the pathogenesis of these complications and finding effective methods to alleviate inflammatory responses is of paramount importance¹.

Ganoderma lucidum is a highly valued medicinal herb in traditional Chinese medicine, renowned for its tonifying and fortifying properties². Polysaccharides, a class of biologically active substances extracted from Ganoderma fungi, have been extensively researched and are considered to possess various health benefits3. Ganoderma lucidum polysaccharides (GIPs) exhibit a range of effects including immunomodulation. antioxidation, anti-inflammation. cardiovascular anti-tumor activity, protection neuroprotection^{4,5}. Inflammation is a physiological defense response of living tissues to harmful stimuli. Ganoderma has shown effective treatment against inflammatory diseases such as acute enteritis, hepatitis and conjunctivitis. Research indicates that *Ganoderma* extracts have a positive effect on capsaicin-induced atopic dermatitis in rats⁶. Nuclear Factor-Kappa B (NF-κB), involved in immune response, inflammatory reactions, cell proliferation and apoptosis, participates in the transcriptional regulation of various inflammatory factor genes. It also regulates the expression level (EL) of a series of inflammation-related genes, thereby increasing the speed of cell apoptosis and promoting neovascular proliferation. The polysaccharides and triterpenoids in Ganoderma work by downregulating or obstructing the TLR/NF-κB and MAPK pathways, ameliorating conditions such as asthma, diabetic nephropathy and others. The NF-κB is involved in the transcriptional regulation of closely associated genes in the body's inflammatory response and immune reactions7. Existing research has demonstrated the close association of activated NF-κB pathways with post-ophthalmic surgical inflammation^{8,9}. Some studies have suggested that GIPs possess notable anti-inflammatory and antioxidant properties¹⁰. These properties position them as potential candidates for treating post-ophthalmic surgical inflammatory responses. The GIPs likely reduce retinal cell inflammation by inhibiting the release of inflammatory mediators and decreasing oxidative stress reactions. The occurrence and progression of inflammatory responses are closely linked to the activation of the NF-κB signaling¹¹. Research suggests that GIPs may regulate inflammatory

responses by inhibiting the activation of the NF- κ B signaling ¹². This mechanism aids in alleviating post-anesthesia inflammation in retinal cells and indicates that GIPs might alleviate inflammation-induced cell damage by promoting cell protection in retinal cells. This includes maintaining cell integrity and function, thereby aiding in preventing cell death.

This study aimed to explore the potential mechanisms by which the natural extract GIPs alleviate inflammation in retinal cells post-ophthalmic anesthesia. By extensively investigating the impact of GIPs on NF- κ B signaling, it aimed to elucidate its potential mechanisms in alleviating inflammation in retinal cells post-anesthesia. Providing critical insights for the exploration of novel therapeutic strategies and intervention methods, this study holds promise in improving the treatment outcomes of post-ophthalmic surgery complications, thereby enhancing ocular health for patients.

MATERIALS AND METHODS

Study area: The study was performed in West China Hospital from October, 2022 to December, 2023.

Fabrication of Ganoderma polysaccharide extract:

Ganoderma lucidum fruiting body powder (Shandong Guanxian Boyide GanodermaCo., Ltd., China) was dehydrated to a constant weight. A 95% ethanol (National Pharmaceutical Group Corporation, China) solution was applied to the dried powder in a liquid-to-material ratio of 20:1 (mL/g). This was intended to eliminate lipids and small molecular impurities by soaking for 24 hrs, repeating the soaking process twice. The resulting residue was obtained after centrifugation, filtered, dried and then stored in a bottle. The alcohol utilized in the pretreatment process was recycled using a rotary evaporator (Shanghai Xinya Pharmaceutical Co., Ltd., China).

The cold-water immersion methodology was employed for extracting GIPs. Specifically, 3 g of defatted *Ganoderma* powder was accurately measured and mixed at an appropriate liquid-to-material ratio. The mixture was soaked at 4°C for 3 min with intermittent stirring, followed by centrifugation (7,656×g, 20 min). The obtained supernatant was filtered and concentrated by rotary evaporation to 25 and 4 mL of the *Ganoderma* aqueous extract was applied to alcohol to achieve a final ethanol concentration of 80%. This solution was refrigerated at 4°C to allow ethanol precipitation. After centrifugation, the resulting precipitate was dissolved in water in a constant temperature incubator (Shanghai Shenteng Company, China) and then adjusted to a final volume of 25 mL in a volumetric flask (Analytik Jena, Germany). This experiment was repeated five times.

Determination of polysaccharide content: Phenol-sulfuric acid method was adopted for total sugar content determination. An 80% phenol solution was prepared and stored in brown bottles at 4°C to avoid light exposure. A 6% phenol solution was made by diluting the 80% phenol solution. Standard curves were generated using various concentrations of standard glucose solution (0~0.1 g/mL). Each was added to test tubes containing the sample solution, followed by 1 mL of 6% phenol (Macklin, China) and 5 mL of concentrated sulfuric acid (Nanjing Chemical Reagent Co., Ltd., China). The reaction mix was placed in a water bath for 15 min, cooled in cold water and the absorbance at 490 nm was measured. A standard curve was constructed and the total sugar content of the samples was calculated using the standard curve equation 13.

The DNS methodology was applied for reducing sugar content determination. Crystalized phenol (13.8 g) was dissolved in 30.4 mL of 10% NaOH solution (Nanjing Chemical Reagent Co., Ltd., China) and water was supplemented to make the volume up to 138 mL. Subsequently, 13.8 g of sodium bisulfite (Changzhou Jiaye Chemical Co., Ltd., China) was applied to the solution to create solution A. A mixture of 510 g of sodium potassium tartrate, dissolved in 600 mL of 10% NaOH solution and 1,760 mL of 1% DNS solution, produced solution B. The AB solution was stored in brown bottles and allowed to stand for a week before use (this mixture serves as the DNS reagent). Various concentrations (0~0.1 mg/mL) of 1 mL standard glucose solutions were applied to test tubes containing the sample solution. To these tubes, 3 mL of DNS reagent was applied and after shaking, they were heated in a boiling water bath for 5 min. After cooling, the solution was adjusted to 25 mL in a volumetric flask and the absorbance was measured at 520 nm to plot a standard curve. The sample's reducing sugar content was calculated using the standard curve equation.

Calculation of polysaccharide content was as follows¹⁴:

Polysaccharide content (%) = Total sugar content (%)-Reducing sugar content (%)

Construction of post-anesthetic retinal cell inflammation model

Animals and grouping: Fifty healthy, specific pathogen-free male Sprague-Dawley (SD) rats (14-18 weeks old, weighing 280-320 g) were selected (purchased from Cavens Laboratory Animals Co., Ltd., China). All rats were housed in an environment with suitable temperature, humidity and lighting and provided with free access to water and food. After an adaptation period of one month, the rats were fed a standard rat diet. The experiment received approval from the Ethical Committee and was conducted in strict compliance with the

regulations of the Laboratory Animal Management Regulations concerning all procedures performed on the animals.

Randomly, fifty specific pathogen-free SD rats were assigned to normal control (C) group, model (M) group, 50+GIP group, 100+GIP group and 150+GIP group, each containing 10 rats. The treatment methods for each group were as follows:

- **Control group:** Healthy SD rats underwent no intervention, serving as the blank control and were maintained under normal breeding conditions. They were orally administered with warm water once daily, at a dosage of 5 mL/kg
- Model group: A retinal detachment model was induced.
 From the day following model establishment, the rats were orally administered with warm water once daily, at a dosage of 5 mL/kg
- **50+GIP group:** Post retinal detachment model induction, the rats were orally administered with a solution of 50 mg/kg GIP once daily, at a dosage of 5 mL/kg
- **100+GIP group:** Post retinal detachment model induction, the rats were orally administered with a solution of 100 mg/kg GIP once daily, at a dosage of 5 mL/kg
- **150+GIP group:** Post retinal detachment model induction, the rats were orally administered with a solution of 150 mg/kg GIP once daily, at a dosage of 5 mL/kg

Following the administration, the rats were observed for half an hour to detect any signs of agitation, breathing difficulties or other abnormalities. No rats died during the administration process.

Construction of retinal detachment model: Three days before surgery, 0.25% chloramphenicol eye drops and 1% atropine eye drops were alternately administered three times a day. On the day of the surgery, the conjunctival sac was rinsed with a physiological saline solution. A 1% lidocaine eye drop wash was performed 2-3 times. All rats underwent the surgical procedure on the right eye. The process involved using 1% atropine for pupil dilation and 10% phenylephrine. Subsequently, a 1 mL/kg injection of 3% Pentobarbital was administered intravenously near the ear. After anesthesia, 0.2 mL of 2% lidocaine was injected subconjunctivally. The nasal side of the conjunctiva and Tenon's fascia were dissected. Subsequently, the sclera at the equator was exposed. A 25-gauge needle was utilized to puncture the sclera 5 mm posterior to the limbus. Then, 0.1 mL of hyaluronidase solution was injected into the central and posterior parts of the vitreous body. After 15 min, another injection was made into the subretinal space. The liquefied

vitreous (0.1 mL) was repeatedly aspirated. Under a microscope and a contact lens, the detachment of the retina was observed, characterized by large gray-white elevations, roughly half the papillary diameter in size. The needle was then withdrawn and aqueous humor was released at the corneal edge. Post-surgery, the conjunctiva was smoothed and a mixture of Gentamicin and Dexamethasone (0.1 mL) was injected subconjunctivally, followed by the application of 0.5% tetracycline eye ointment in the conjunctival sac. To prevent infection, a muscular injection of 8,000 μ Gentamicin was administered. For a week post-surgery, the rats received chloramphenicol eye drops four times a day and continued to use 1% atropine eye drops for pupil dilation.

Sample collection: The retinal specimen was collected as follows. Five randomly selected rats from each group were anesthetized and secured on a dissection board. The rats' lateral canthus and conjunctiva were sequentially cut and the episclera was separated. After the extraocular muscles were partially dissected, the eye was removed by cutting the optic nerve. The extracted eyeball was rapidly placed on ice. Under a microscope, the cornea, lens and most of the vitreous were removed. The glassy retina was positioned in a 1.5 mL Eppendorf tube, submerged in liquid nitrogen for 10 min and then stored in a -80°C freezer for future use. Each group's retinal samples were processed to create pathological specimens for apoptotic cell analysis.

The serum sample was collected as follows. Rats were positioned supine and after the removal of the eyeballs, the limbs were secured with needles. Using 75% alcohol for disinfection, an incision was made in the subcutaneous tissue along the abdominal midline, allowing blunt dissection to the bilateral kidneys. After the abdominal aorta was located, arterial blood was drawn. After centrifugation at 1,000 r/min for 5 min, the supernatant was collected and stored in -80°C freezer for future use.

In vivo experimental evaluation indicators

Retinal electrophysiological testing: Following the completion of the experimental procedures, retinal function was evaluated using the GT-2000NV visual electrophysiological system (Electroretinogram, ERG) in rats. The rats were secured onto a testing board during the assessment. Silver needles were utilized to form recording electrodes and reference electrodes, inserted into the corneal stroma and forehead skin, respectively. A grounding electrode was inserted into the posterior skin. Before the experiment, rats were administered 1% tropicamide to induce mydriasis, adapted to darkness for half an hour, one eye was covered and subsequently, the visual electrophysiological apparatus was

utilized to record the amplitude of a-waves and b-waves in the rat's retinal electrophysiology, both at twelve hours and one week after the procedures.

Measurement of retinal thickness: The bilateral eyeballs from each group of rats were collected and the vitreous body and crystalline lens were extracted. The retinal tissues were preserved at -80°C for subsequent use. One portion of the retinal tissue was prepared for Western blot analysis, while the other eyeball was immersed in 10% formalin overnight for the preparation of pathological sections. Hematoxylin and Eosin (H&E) staining was performed on the retinal tissues and their morphological characteristics were visualized under a microscope. By making incisions along the optic nerve axis of the formalin-fixed eyeballs, the central area of the retina was exposed to measure the retinal thickness. The measurement of total thickness extended from the inner limiting membrane to the retinal pigment epithelium. For the measurement of the outer retinal thickness, the evaluation extended from the outer plexiform layer to the outer nuclear layer.

Measurement of VEGF levels: Vascular Endothelial Growth Factor (VEGF) levels in rat serum were assessed using Enzyme Linked Immunosorbent Assay (ELISA) (Sigma-Aldrich, USA). The ELISA kit was allowed to equilibrate at 25°C for 30 min. Sample thawing was performed at 4°C, followed by centrifugation at 12,000 rpm for 5 min according to the instructions provided in the assay kit. The control standard working solution (100 µL) was applied, along with the test samples (100 µL) to other wells and the plate was incubated with a cover for 90 min. The liquid was discarded by inverting and tapping the plate. Each well was washed with 300 µL of wash solution and left to rest for 2 min and the solution was then discarded by tapping and inverting the plate; this process was repeated five times. The TMB One-Step Substrate Reagent solution (100 µL) was applied to each well and the plate was gently shaken at 25°C in the dark for 30 min. The plate was washed 3 times with 350 µL of wash solution. Enzyme-conjugate working solution (100 µL) was applied to each well, covered and incubated at the appropriate temperature for 30 min. The plate was washed five times. Substrate solution (90 µL) was applied and the plate was covered and incubated in the dark for 15 min. Finally, 50 µL of stop solution was applied to halt the reaction. The optical density (OD value) of each well was measured at a wavelength of 450 nm using an ELISA reader within 5 min after the reaction was stopped.

Measurement of inflammatory factors in rat retinas: The levels of inflammation-related factors (TNF- α , IL-1 β , IL-6, ICAM-1 and IL-18) in rat serum were assessed via ELISA.

The ELISA kit was allowed to equilibrate at 25°C for 30 min. Samples were thawed at 4°C and then centrifuged at 12,000 rpm for 5 min. Following the preparation of the standard curve gradients and standard dilutions, 100 µL of the sample was applied to each well of the ELISA plate. The plate was subjected to gentle shaking for 2 min using a microplate shaker (Shanghai Jingxin Industrial Development Co., Ltd., China), sealed and incubated for 2 hrs. The liquid was discarded and the plate was tapped dry, followed by multiple washes by adding wash solution, inverting and tapping; this process was repeated five times. Subsequently, 100 µL of biotin-labeled antibodies were applied, sealed and incubated for 1 hr. The liquid was discarded and the plate was tapped dry and washed multiple times. In each well, 100 µL of working solution and HRP were applied and incubated at 25°C for half an hour. After the liquid was discarded, the plate was tapped dry and washed several times. Then, 100 µL of substrate solution was applied to each well, left to develop color at 25 °C in the dark for half an hour, followed by the addition of 100 µL of stop solution. The measurement methodology for OD value was the same as in the previous section.

Retinal cell culture: Retinal cells were cultured using DMEM+10% fetal bovine serum. The medium in the 6-well culture plate was supplemented with antibiotics and antifungal agents to prevent bacterial and fungal contamination. A layer of extracellular matrix proteins like collagen or gelatin was coated in the culture dish to assist the cells in adapting to the environment of a cell culture chamber set at 37°C, 5% CO₂ and 95% relative humidity. Cells in the logarithmic growth phase were randomly rolled into various groups, with each group having nine replicate wells. The C group was untreated. The M group consisted of cells from the above rat model. For 50+GIP group, cells were cultured in a medium with 5 µg/mL of GIPs. The 100+GIP group was cultured in a medium containing 10 µg/mL of GIPs and 150+GIP group was cultured in a medium containing 15 µg/mL of GIPs. The cells were stimulated for 24 hrs and at the end of the experiment, the cells were collected.

In vitro experimental evaluation indexes

Detection of apoptosis-related protein EL in rat retinal

tissues: The protein immunoblotting (Western blot) assay was employed to detect the EL of apoptosis-related proteins Bcl-2/Bax in the retinal tissues of the various groups of rats. Retinal tissues from each group of rats were utilized and protein extraction was carried out using RIPA lysis buffer. Bradford protein assay was utilized to determine the protein

content and 50 μ g of the protein was electrophoresed and transferred onto a PVDF membrane (Arkema, France). Following blocking with BSA (Bovine Serum Albumin) (Procell Life Technologies Co., Ltd., China), incubation with primary antibodies (Sigma-Aldrich Company) was carried out at 4°C, followed by secondary antibodies (Sigma-Aldrich Company) tagged with HRP (Macklin, China) and incubation at 37°C for 1 hr. The β -actin was utilized as an internal control and the relative EL of the target protein was determined by the ratio of integrated optical density to β -actin.

The Caspase-3 protein ELs were assessed using an ELISA kit. Protein extraction was performed using RIPA (Macklin, China) lysis buffer and the protein content was determined using the Bradford methodology. The spectrophotometric absorbance of the samples was measured at 450 nm using an ELISA reader (Shanghai Enzyme-linked Biotechnology Co., Ltd., China).

Measurement of NF-κB signaling-related protein mRNA EL:

Real-time PCR was utilized. Gene sequences were obtained from GenBank. Retinal cell total RNA was extracted using Trizol, where each sample utilized 1 mL of Trizol reagent and 0.2 mL of chloroform. The mixture was centrifuged at 4°C, 12,000 rpm, for 20 min. The PCR reaction system totaled 20.0 µL, composed of 10.0 µL 2×SybrGreen Qpcr Master Mix, 2.0 µL template cDNA, 0.4 µL 10 µmol/L PCR forward primer, 0.4 µL 10 µmol/L PCR reverse primer and 7.2 µL ddH₂O. The reaction conditions involved an initial denaturation at 95°C for 3 min followed by 45 cycles of denaturation at 95°C for 7 sec, annealing at 55°C for 10 sec and extension at 72°C for 15 sec. The housekeeping gene, β -tain, was utilized as an internal reference and the data was analyzed according to the $2^{-\Delta\Delta Ct}$ method Maren *et al.*15.

The primer sequences for the upstream and downstream regions of the genes were as follows:

- For NF-κB: Upstream sequence: 5'-GGAGACTCACTTTCT TGGGGAC-3', downstream sequence: 5'-ATTCGCTTTGCCTTC CTCC-3'
- For LOX-1: Upstream sequence: 5'-TCCAAAGTCTCCCAACC AAC-3', downstream sequence: 5'-GTCTTTCATGCGGCAA CAG-3'
- For TRAF-6: Upstream sequence: 5'-TCTGCTTGATGGC TTTACGG-3', downstream sequence: 5'-TTACCGTCAGGG AAAGAATCTC-3'
- For TLR-4: Upstream sequence: 5'-TGGTTTACAC GTCCATCGGT-3', downstream sequence: 5'-ATCAATGGTC ACATCACATAGTCC-3'

Statistical methods: Each experiment was repeated three times and all experimental data were statistically analyzed employing SPSS 23.0. Mean \pm Standard Deviation ($\overline{\chi}\pm$ s) was how measurement data were denoted. The differences between two independent samples were compared using Student's t-test and differences among multiple groups were compared using one-way analysis of variance. A significance level of p<0.05 was set to define statistically considerable differences.

RESULTS

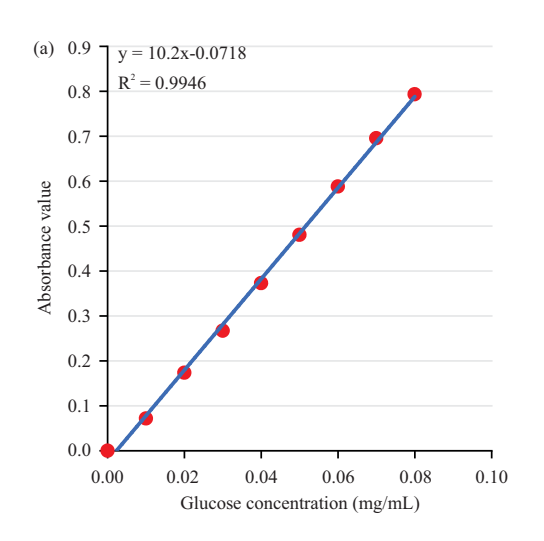
Ganoderma polysaccharide extraction results: The cold-water immersion methodology was utilized for extracting GIPs. The results displayed a strong linear relationship in both the total sugar equation y = 10.2x-0.0718 ($R^2 = 0.9946$) and the reducing sugar equation y = 10.04x-0.0464 ($R^2 = 0.9973$)

(Fig. 1a-b). In Fig. 2, the five extraction repetitions resulted in GIP content of 39.34, 38.69, 39.71, 38.97 and 38.91%, respectively.

In vivo experimental results

Effect of GIP on rat retinal electroretinogram amplitudes: In

Fig. 3, compared to the C group, the amplitude levels of both a-waves and b-waves in the rat retinas in the M group were significantly reduced (p<0.05). In contrast to the M group, the amplitude levels of retinal a-waves and b-waves in the 50+GIP group, 100+GIP group and 150+GIP group rats were significantly increased 24 hrs (Fig. 3a) and 1 week (Fig. 3b) after treatment (p<0.05). Among the 50+GIP group, 100+GIP group and 150+GIP group, the amplitude levels of retinal a-waves and b-waves in the 150+GIP group rats were significantly the highest 24 hrs and 1 week after treatment (p<0.05).



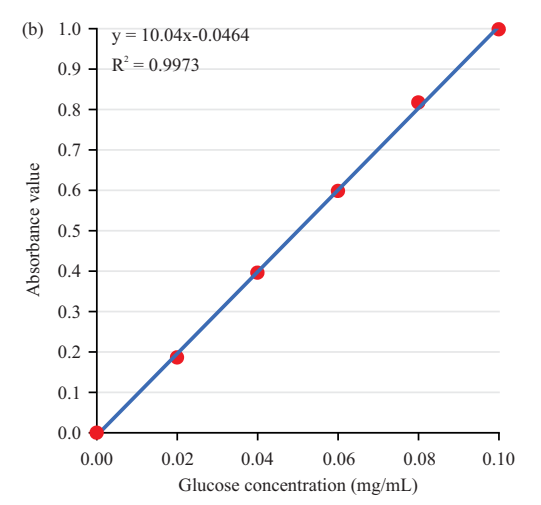


Fig. 1(a-b): Standard curve, (a) Total sugar and (b) Reducing sugar

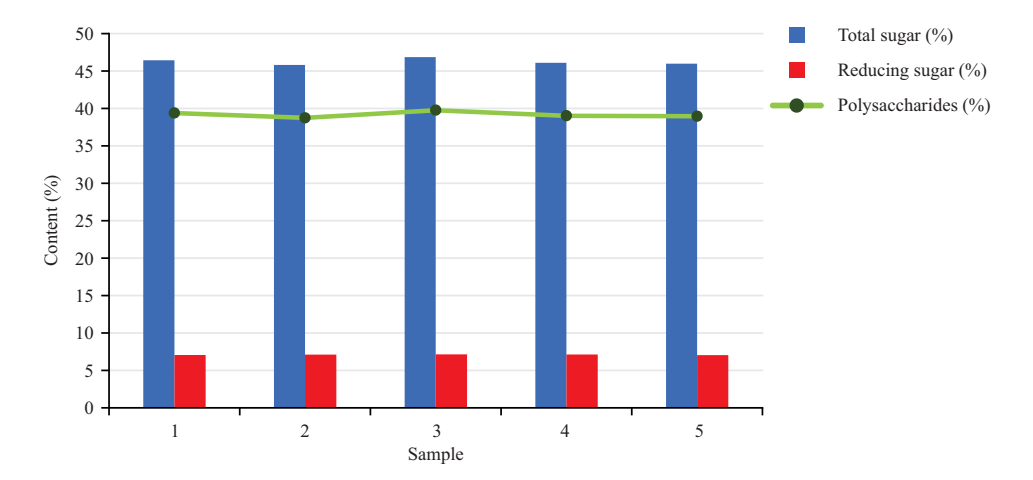


Fig. 2: Analysis of GIP extraction results

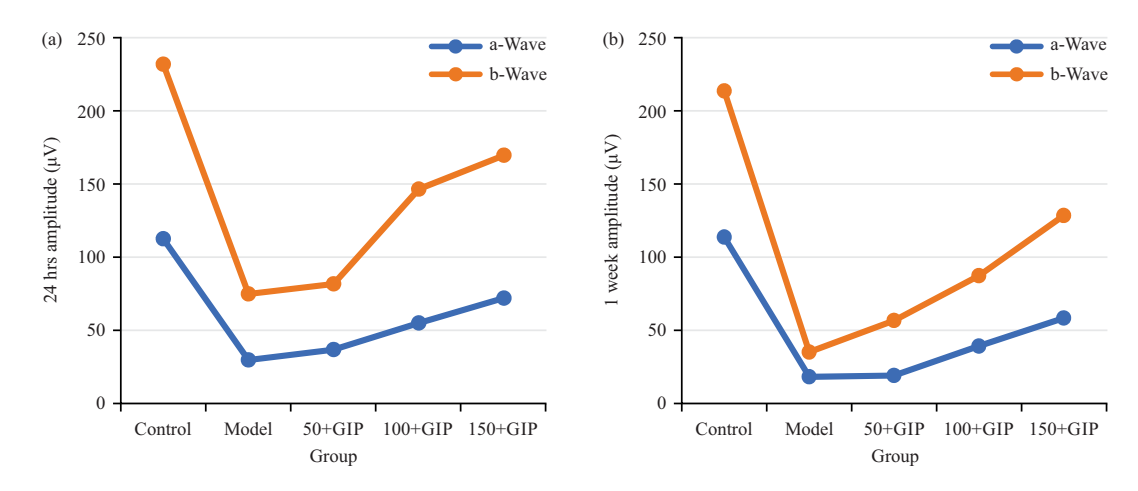


Fig. 3(a-b): Influence of GIP on the retinal electroretinogram amplitudes in rats, (a) 24 hrs and (b) 1 week

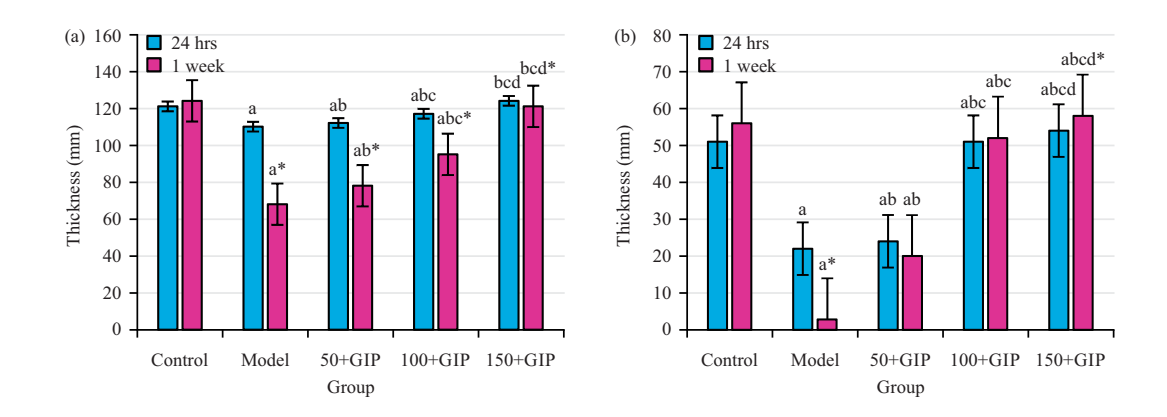


Fig. 4(a-b): Result of, (a) Full thickness and (b) Half thickness

*p<0.05 vs 24 hrs, ap<0.05 vs C group, p<0.05 vs M group, p<0.05 vs 50+GIP group and p<0.05 vs 100+GIP group

Retinal thickness results in rats: As illustrated in Fig. 4, compared to the C group, the total retinal thickness and outer layer thickness in rat retinas in the M group were significantly decreased (p<0.05). In contrast to the model group, the total retinal thickness (Fig. 4a) and outer layer thickness (Fig. 4b) in the 50+GIP group, 100+GIP group and 150+GIP group rats were significantly increased 24 hrs and 1 week after treatment (p<0.05). Among the 50+GIP group, 100+GIP group and 150+GIP group, the total retinal thickness and outer layer thickness in the 150+GIP group rats were significantly the highest 24 hrs and 1 week after treatment (p<0.05).

Inflammatory factor detection results: Figure 5 demonstrated the detection results of inflammatory factors. It revealed that, compared to the C group, the levels of VEGF (Fig. 5a-f) in the rat retinas in the M group significantly increased (p<0.05). In contrast to the M group, the levels of VEGF, TNF- α , IL-1 β , IL-6, ICAM-1 and IL-18 in the 50+GIP group,

100+GIP group and 150+GIP group rats were significantly decreased 24 hrs and 1 week after treatment, showing great significances (p<0.05). Additionally, after 1 week of treatment, the levels of VEGF, TNF- α , IL-1 β , IL-6, ICAM-1 and IL-18 in the 50+GIP group, 100+GIP group and 150+GIP group rats were significantly lower than those at 24 hrs (p<0.05). Among the 50+GIP group, 100+GIP group and 150+GIP group, the levels of VEGF, TNF- α , IL-1 β , IL-6, ICAM-1 and IL-18 in the 150+GIP group rats were significantly the lowest 24 hrs and 1 week after treatment (p<0.05).

In vitro experiment results

Retinal cell proliferation test results: In the *in vitro* cell experiment, C group showed no remarkable changes, while M group exhibited inhibited retinal cell proliferation. With the increase in the duration of treatment with GIPs (50+GIP group, 100+GIP group and 150+GIP group), apoptosis of cells was inhibited and the apoptosis rate decreased gradually.

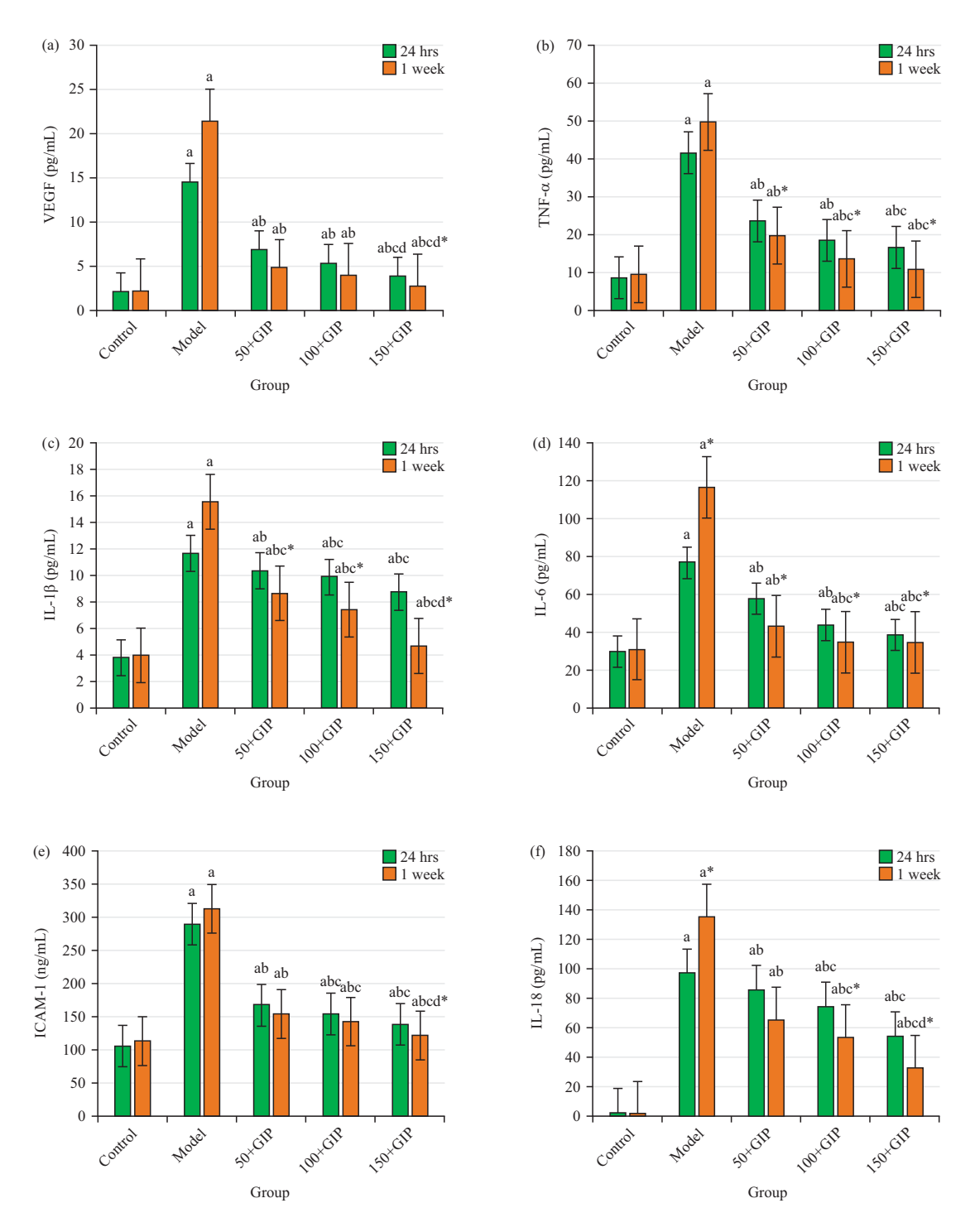


Fig. 5(a-f): Comparison of VEGF levels among various groups, levels of (a) VEGF, (b) TNF- α , (c) IL-1 β , (d) IL-6, (e) ICAM-1 and (f) IL-18, respectively

*p<0.05 vs 24 hrs, a p<0.05 vs C group, b p<0.05 vs M group, c p<0.05 vs 50+GIP group and d p<0.05 vs 100+GIP group

A substantial difference was observed between C and M groups (p<0.05). Additionally, 50+GIP group, 100+GIP group and 150+GIP group showed substantial differences versus M group (p<0.05) (Fig. 6).

Results of apoptosis-related protein detection: As illustrated in Fig. 7, compared to the C group, the expression levels of Bcl-2 (Fig. 7a) protein in the rat retinas in the M group significantly decreased, while the expression levels of Bax-2

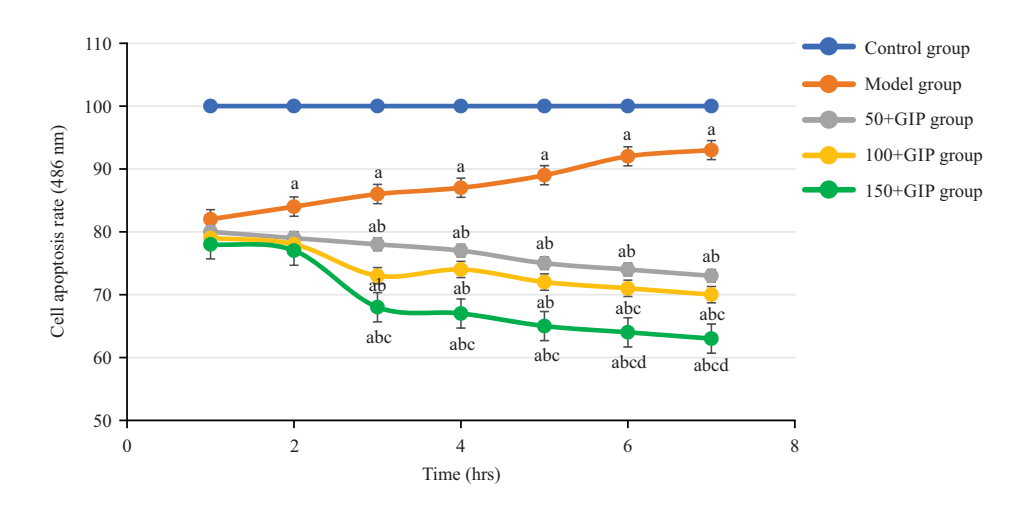


Fig. 6: Results of retinal cell proliferation *in vitro*^ap<0.05 vs C group, ^bp<0.05 vs M group, ^cp<0.05 vs 50+GIP group and ^dp<0.05 vs 100+GIP group

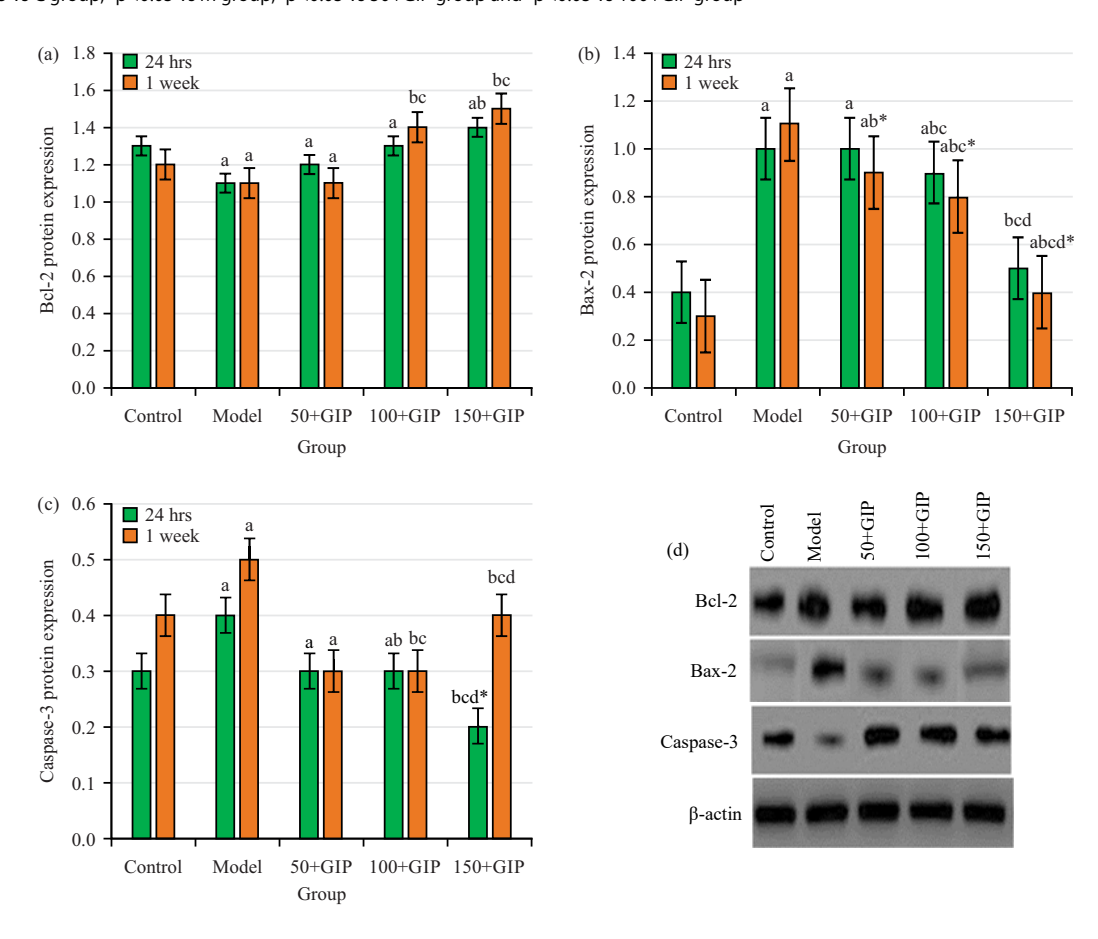


Fig. 7(a-d): Comparison of protein levels in various groups, (a) Bcl-2, (b) Bax-2, (c) Caspase-3 and (d) WB bands ^ap<0.05 vs C group, ^bp<0.05 vs M group, ^cp<0.05 vs 50+GIP group and ^dp<0.05 vs 100+GIP group

(Fig. 7b) and Caspase-3 (Fig. 7c) proteins sharply increased (p<0.05). In comparison to the M group, the expression levels of Bcl-2 protein in the 50+GIP group, 100+GIP group and 150+GIP group rats were significantly increased, while the

expression levels of Bax and Caspase-3 proteins were substantially decreased 24 hrs and 1 week after treatment (p<0.05). After 1 week of treatment, the expression levels of Bcl-2 protein in the 50+GIP group, 100+GIP group and

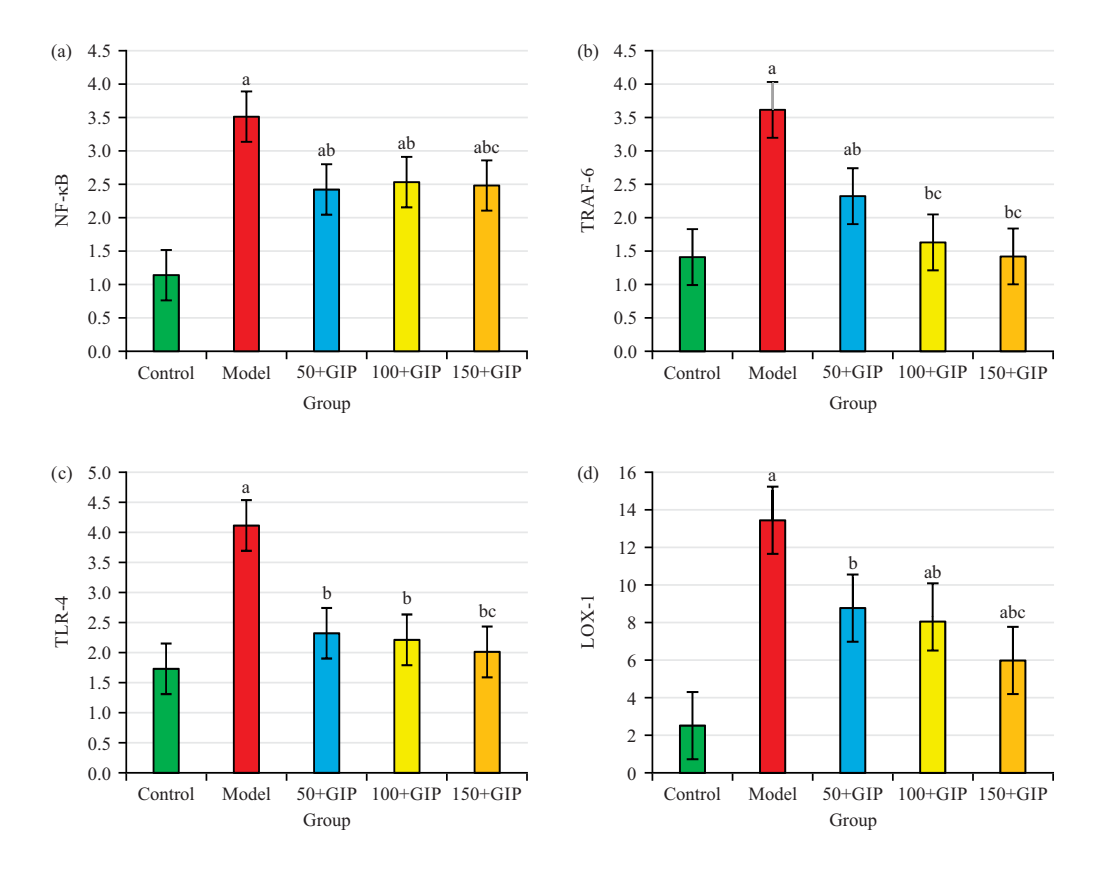


Fig. 8(a-d): Relative mRNA ELs in various groups, (a) NF-kB, (b) TRAF-6, (c) TLR-4 and (d) LOX-1 ^ap<0.05 vs C group, ^bp<0.05 vs M group and ^cp<0.05 vs 50+GIP group

150+GIP group rats were significantly higher when compared to those at 24 hrs, while the expression levels of Bax and Caspase-3 proteins were significantly lower than those at 24 hrs (p<0.05). The WB band was shown in Fig. 7d.

NF-κB pathway-related mRNA ELs: As explicated in Fig. 8, compared to the C group, the expression levels of NF-κB (Fig. 8a), TRAF-6 (Fig. 8b), TLR-4 (Fig. 8c) and LOX-1 (Fig. 8d) in rat retinas in the M group significantly increased (p<0.05). In contrast to the M group, the expression levels of NF-κB, TRAF-6, TLR-4 and LOX-1 in the 50+GIP group, 100+GIP group and 150+GIP group rats were significantly decreased (p<0.05).

DISCUSSION

During some ophthalmic surgeries, anesthesia is administered. However, some patients may experience symptoms such as blurred vision and eye irritation after anesthesia, possibly due to factors like corneal swelling and in severe cases, it may lead to epithelial detachment¹⁶. *Ganoderma* polysaccharides, as one of the effective components in *Ganoderma* (Reishi mushroom), possess

diverse pharmacological activities. These include enhancing the body's immune system, scavenging free radicals, anti-radiation effects, anti-tumor properties and promoting longevity¹⁷⁻¹⁹. Additionally, *Ganoderma* polysaccharides have been shown to lower blood pressure, reduce blood lipids and improve blood circulation²⁰. In this study, *Ganoderma* polysaccharides were extracted using a cold-water soaking method. It was observed that during the extraction process, the concentrations of total sugars and reducing sugars in *Ganoderma* increased linearly with the increase in glucose concentration.

External impacts and eyeball deformation caused by severe myopia can potentially lead to retinal damage and tears²¹. Retinal damage, thinning and detachment are major pathological characteristics of retinal injuries²². This study found that after treatment with *Ganoderma* polysaccharides, the amplitude of the electroretinogram and the thickness of the retina in rats with anesthetized retinal injury significantly increased. This suggests that *Ganoderma* polysaccharides can improve the extent of retinal damage caused by anesthesia to some extent. Subsequently, this study investigated the changes in levels of VEGF, TNF-α, IL-1β, IL-6, ICAM-1 and IL-18

in rats with anesthetized retinal injury. The VEGF plays a role in inducing retinal neovascularization and enhancing vascular permeability, being a significant factor in vitreous hemorrhage and tractional retinal detachment²³. The TNF- α is a crucial inflammatory mediator in inflammatory reactions, playing a vital role in activating endothelial cells and chemotaxis of neutrophils²⁴. The IL-1B, secreted by activated antigenpresenting cells, can induce the production of factors such as TNF- α and IL-6, exacerbating tissue damage²⁵. Excessive expression of TNF- α and IL-1 β in retinal diseases can trigger inflammation, leading to damage to retinal tissues²⁶. The ICAM-1 is expressed on endothelial cells under inflammatory conditions, aiding in leukocyte adhesion and migration of inflammatory cells. In retinal diseases, upregulation of ICAM-1 may be associated with inflammation and vascular pathology²⁷. This study found an increase in levels of VEGF, TNF- α , IL-1 β , IL-6, ICAM-1 and IL-18 in the rat model of retinal injury, while levels of these factors decreased after treatment with Ganoderma polysaccharides. Meng et al.28 found that Ganoderma polysaccharides could decreased the production of IL-1β, IL-6 and TNF-α in rheumatoid arthritis, exhibiting anti-inflammatory effects. Gokce et al.29 discovered that polysaccharides could reduce inflammation by lowering TNF- α and NO levels in traumatic spinal cord injury tissue, facilitating tissue recovery. This indicates that Ganoderma polysaccharides can alleviate the inflammatory damage induced by anesthesia by reducing the expression of inflammatory factors.

To further investigate the protective effects of Ganoderma polysaccharides on retinal damage, this study analyzed their impact on retinal cell proliferation and apoptosis, revealing a decrease in the apoptosis rate of retinal cells after treatment. The Bcl-2 is an anti-apoptotic protein and its overexpression in retinal tissue damage diseases may contribute to maintaining the survival of retinal cells and alleviating cell death³⁰. The Bax is a pro-apoptotic protein and an increase in Bax expression levels can induce cell apoptosis and exacerbate tissue damage³¹. The Caspase-3 is a key executor of cell apoptosis, mediating the degradation of nuclear DNA and cell breakdown during the apoptosis process³². The study found that after treatment with Ganoderma polysaccharides, the expression levels of Bcl-2 protein increased, while the expression levels of Bax and Caspase-3 proteins decreased in retinal injury cells. This indicates that Ganoderma polysaccharides can inhibit apoptosis in retinal cells after injury by regulating the expression of pro-apoptotic and anti-apoptotic proteins. The NF-κB is involved in various cell signaling pathways, including immune and inflammatory responses. Aberrant

activation of NF-κB may lead to the release of inflammatory factors such as TNF-α and IL-1β, triggering an inflammatory response³³. Studies have shown a close relationship between abnormal NF-κB activation and the progression of retinal inflammatory injury³⁴. Additionally, TRAF-6, TLR-4 and LOX-1 are all related to inflammatory responses. Studies have indicated that diabetic retinopathy patients often exhibit upregulation of TRAF-2 and TRAF-6 in endothelial cells and Müller cells and this signaling pathway may be involved in promoting retinal inflammation in diabetic retinopathy patients³⁵. Seidel et al.³⁶ found that TLR4 deficiency in retinal endothelial cells could prevent diabetes-induced increases in retinal permeability, neuronal damage and vascular injury, although its role in Müller cells was less apparent. Gao et al.³⁷ demonstrated that LOX-1 expression increased in lightinduced retinal degeneration and inhibiting LOX-1 expression could suppress inflammation and cell death in retinal degeneration while reducing the neurotoxic effects of glial cells on photoreceptor cells. The study found that after treatment with Ganoderma polysaccharides, the expression levels of NF-κB. TRAF-6. TLR-4 and LOX-1 decreased in retinal injury cells. This indicates that *Ganoderma* polysaccharides can improve the process of retinal damage by regulating the expression of NF-κB, TRAF-6, TLR-4 and LOX-1.

CONCLUSION

The results indicated that the cold-water extraction methodology is effective in extracting GIPs, showing repeatability and reliability. The GIPs considerably alleviated the inflammatory response of retinal cells after anesthesia, suppressed the EL of inflammatory factors and inhibited cell apoptosis. This process might be achieved by modulating the ELs of proteins associated with the NF- κ B signaling. Although, the research results suggest that GIPs might mitigate the inflammatory response by regulating the NF- κ B signaling, the specific molecular mechanism requires further in-depth investigation. Further research can explore how GIPs influence the various components of NF- κ B signaling. A comprehensive study of GIPs will help reveal their mechanisms of action, offering clinical evidence for the treatment of retinal diseases.

SIGNIFICANCE STATEMENT

This study investigated the mechanism by which *Ganoderma lucidum* polysaccharides modulates postanesthesia retinal cell inflammation, revealing its potential to alleviate inflammation by regulating the NF-κB signaling pathway. The results demonstrated that *Ganoderma lucidum* polysaccharides effectively inhibited retinal cell inflammation,

providing a basis for developing novel anti-inflammatory treatments. This expands academic understanding of ophthalmic complications post-anesthesia and the application of natural extracts in inflammation therapy.

REFERENCES

- Britten-Jones, A.C., R. Jin, S.A. Gocuk, E. Cichello and F. O'Hare et al., 2022. The safety and efficacy of gene therapy treatment for monogenic retinal and optic nerve diseases: A systematic review. Genet. Med., 24: 521-534.
- Hsieh, T.C. and J.M. Wu, 2011. Suppression of proliferation and oxidative stress by extracts of *Ganoderma lucidum* in the ovarian cancer cell line OVCAR-3. Int. J. Mol. Med., 28: 1065-1069.
- 3. Shi, Y.J., H.X. Zheng, Z.P. Hong, H.B. Wang, Y. Wang, M.Y. Li and Z.H. Li, 2021. Antitumor effects of different *Ganoderma lucidum*spore powder in cell- and zebrafish-based bioassays. J. Integr. Med., 19: 177-184.
- 4. Li, Z., Y. Shi, X. Zhang, J. Xu, H. Wang, L. Zhao and Y. Wang, 2020. Screening immunoactive compounds of *Ganoderma lucidum* spores by mass spectrometry molecular networking combined with *in vivo* zebrafish assays. Front. Pharmacol., Vol. 11. 10.3389/fphar.2020.00287.
- 5. Zhao, D., M.W. Chang, J.S. Li, W. Suen and J. Huang, 2014. Investigation of ice-assisted sonication on the microstructure and chemical quality of *Ganoderma lucidum* spores. J. Food Sci., 79: E2253-E2265.
- Li, C., J.H. Kim, B.U. Ji, J.E. Lee and Y. Kim *et al.*, 2015. Inhibitory
 effects of *Ganoderma lucidum* pharmacopuncture on atopic
 dermatitis induced by capsaicin in rats. J. Dermatological Sci.,
 80: 212-214.
- Smina, T.P., S. De, T.P.A. Devasagayam, S. Adhikari and K.K. Janardhanan, 2011. *Ganoderma lucidum* total triterpenes prevent radiation-induced DNA damage and apoptosis in splenic lymphocytes *in vitro*. Mutat. Res. Genet. Toxicol. Environ. Mutagen., 726: 188-194.
- González, A., V. Atienza, A. Montoro and J.M. Soriano, 2020. Use of *Ganoderma lucidum* (Ganodermataceae, Basidiomycota) as radioprotector. Nutrients, Vol. 12. 10.3390/nu12041143.
- 9. Jin, X., J.R. Beguerie, D.M.Y. Sze and G.C.F. Chan, 2012. *Ganoderma lucidum* (Reishi mushroom) for cancer treatment. Cochrane Database Syst. Rev., Vol. 4. 10.1002/14651858.CD007731.pub2.
- 10. Ahmad, M.F., 2020. *Ganoderma lucidum*. A rational pharmacological approach to surmount cancer. J. Ethnopharmacol., Vol. 260. 10.1016/j.jep.2020.113047.

- 11. Xu, J., C. Xiao, H. Xu, S. Yang and Z. Chen *et al.*, 2021. Anti-inflammatory effects of *Ganoderma lucidum* sterols via attenuation of the p38 MAPK and NF-κB pathways in LPS-induced RAW 264.7 macrophages. Food Chem. Toxicol., Vol. 150. 10.1016/j.fct.2021.112073.
- Zhong, L., P. Yan, W.C. Lam, L. Yao and Z. Bian, 2019. Coriolus versicolor and Ganoderma lucidum related natural products as an adjunct therapy for cancers: A systematic review and meta-analysis of randomized controlled trials. Front. Pharmacol., Vol. 10. 10.3389/fphar.2019.00703.
- Zhang, X., W. Wei, G. Tao, Q. Jin and X. Wang, 2022. Triacylglycerol regioisomers containing palmitic acid analyzed by ultra-performance supercritical fluid chromatography and quadrupole time-of-flight mass spectrometry: Comparison of standard curve calibration and calculation equation. Food Chem., Vol. 391. 10.1016/j.foodchem.2022.133280.
- Ruizuo, S., N. Tiegui, Y. Zuo, J. Yan, Y. Quan, Z. Min and H. Kaiyong, 2019. Study on the content of polysaccharide from different origins and the monosaccharide composition of polysaccharide. China J. Chin. Materia Medica, 44: 3608-3614.
- Maren, N.A., J.R. Duduit, D. Huang, F. Zhao, T.G. Ranney and W. Liu, 2023. Stepwise Optimization of Real-Time RT-PCR Analysis. In: Plant Genome Engineering: Methods and Protocols, Yang, B., W. Harwood and Q. Que (Eds.), Humana, New York, ISBN: 978-1-0716-3131-7, pp: 317-332.
- 16. Pucchio, A., D.R. Pur, A. Dhawan, S.K. Sodhi, A. Pereira and N. Choudhry, 2023. Anesthesia for ophthalmic surgery: An educational review. Int. Ophthalmol., 43: 1761-1769.
- 17. Seweryn, E., A. Ziała and A. Gamian, 2021. Health-promoting of polysaccharides extracted from *Ganoderma lucidum*. Nutrients, Vol. 13. 10.3390/nu13082725.
- Zhang, X., D. Wu, Y. Tian, X. Chen and J. Lan et al., 2022. Ganoderma lucidum polysaccharides ameliorate lipopolysaccharide-induced acute pneumonia via inhibiting NRP1-mediated inflammation. Pharm. Biol., 60: 2201-2209.
- Ahmad, R., M. Riaz, A. Khan, A. Aljamea, M. Algheryafi, D. Sewaket and A. Alqathama, 2021. *Ganoderma lucidum* (Reishi) an edible mushroom; a comprehensive and critical review of its nutritional, cosmeceutical, mycochemical, pharmacological, clinical, and toxicological properties. Phytother. Res., 35: 6030-6062.
- Kou, F., Y. Ge, W. Wang, Y. Mei and L. Cao et al., 2023. A review of Ganoderma lucidum polysaccharides: Health benefit, structure-activity relationship, modification, and nanoparticle encapsulation. Int. J. Biol. Macromol., Vol. 243. 10.1016/j.ijbiomac.2023.125199.
- 21. Bhavsar, K.V., Z. Michel, M. Greenwald, E.T. Cunningham Jr. and K.B. Freund, 2021. Retinal injury from handheld lasers: A review. Surv. Ophthalmol., 66: 231-260.

- 22. Guttenplan, K.A., B.K. Stafford, R.N. El-Danaf, D.I. Adler and A.E. Münch *et al.*, 2020. Neurotoxic reactive astrocytes drive neuronal death after retinal injury. Cell Rep., Vol. 31. 10.1016/j.celrep.2020.107776.
- Rangel, B., L.A. Mesentier-Louro, L.L. Lowe, A.M. Shariati, R. Dalal, J.A. Imventarza and Y.J. Liao, 2022. Upregulation of retinal VEGF and connexin 43 in murine nonarteritic anterior ischemic optic neuropathy induced with 577 nm laser. Exp. Eye Res., Vol. 225. 10.1016/j.exer.2022.109139.
- 24. Yu, Z., Y. Wen, N. Jiang, Z. Li and J. Guan *et al.*, 2022. TNF-α stimulation enhances the neuroprotective effects of gingival MSCs derived exosomes in retinal ischemia-reperfusion injury via the MEG3/miR-21a-5p axis. Biomaterials, Vol. 284. 10.1016/j.biomaterials.2022.121484.
- 25. Xie, Z., Q. Ying, H. Luo, M. Qin and Y. Pang *et al.*, 2023. Resveratrol alleviates retinal ischemia-reperfusion injury by inhibiting the NLRP3/Gasdermin D/Caspase-1/Interleukin-1β pyroptosis pathway. Invest. Ophthalmol. Visual Sci., Vol. 64. 10.1167/jovs.64.15.28.
- 26. Bian, Z.M., S.G. Elner, R.M. Strieter, S.L. Kunkel, N.W. Lukacs and V.M. Elner, 1999. IL-4 potentiates IL-1β- and TNF-a-stimulated IL-8 and MCP-1 protein production in human retinal pigment epithelial cells. Curr. Eye Res., 18: 349-357.
- 27. Lee, D., and H.S. Hong, 2023. Substance P alleviates retinal pigment epithelium dysfunction caused by high glucose-induced stress. Life, Vol. 13. 10.3390/life13051070.
- 28. Meng, M., L. Wang, Y. Yao, D.M. Lin and C. Wang *et al.*, 2023. *Ganoderma lucidum* polysaccharide peptide (GLPP) attenuates rheumatic arthritis in rats through inactivating NF-κB and MAPK signaling pathways. Phytomedicine, Vol. 119. 10.1016/j.phymed.2023.155010.
- 29. Gokce, E.C., R. Kahveci, O.M. Atanur, B. Gürer and N. Aksoy *et al.*, 2015. Neuroprotective effects of *Ganoderma lucidum* polysaccharides against traumatic spinal cord injury in rats. Injury, 46: 2146-2155.

- 30. Orieux, G., L. Picault, A. Slembrouck, J.E. Roger and X. Guillonneau *et al.*, 2014. Involvement of Bcl-2-associated transcription factor 1 in the differentiation of early-born retinal cells. J. Neurosci., 34: 1530-1541.
- 31. Risner, M.L., S. Pasini, N.R. McGrady and D.J. Calkins, 2022. *Bax* contributes to retinal ganglion cell dendritic degeneration during glaucoma. Mol. Neurobiol., 59: 1366-1380.
- 32. Suo, L., C. Liu, Q.Y. Zhang, M.D. Yao and Y. Ma *et al.*, 2022. METTL3-mediated *M*-methyladenosine modification governs pericyte dysfunction during diabetes-induced retinal vascular complication. Theranostics, 12: 277-289.
- 33. Laczko, R., A. Chang, L. Watanabe, M. Petelo, K. Kahaleua, J.P. Bingham and K. Csiszar, 2020. Anti-inflammatory activities of *Waltheria indica* extracts by modulating expression of IL-1B, TNF-α, TNFRII and NF-κB in human macrophages. Inflammopharmacology, 28: 525-540.
- 34. Mirra, S., L. Sánchez-Bellver, C. Casale, A. Pescatore and G. Marfany, 2022. Ubiquitin specific protease USP48 destabilizes NF-κB/p65 in retinal pigment epithelium cells. Int. J. Mol. Sci., Vol. 23. 10.3390/ijms23179682.
- 35. Vos, S., R. Aaron, M. Weng, J. Daw, E. Rodriguez-Rivera and C.S. Subauste, 2023. CD40 upregulation in the retina of patients with diabetic retinopathy: Association with TRAF2/TRAF6 upregulation and inflammatory molecule expression. Invest. Ophthalmol. Visual Sci., Vol. 64. 10.1167/iovs.64.7.17.
- 36. Seidel, A., L. Liu, Y. Jiang and J.J. Steinle, 2021. Loss of TLR4 in endothelial cells but not Müller cells protects the diabetic retina. Exp. Eye Res., Vol. 206. 10.1016/j.exer.2021.108557.
- 37. Gao, X., R. Zhu, J. Du, W. Zhang, W. Gao and L. Yang, 2020. Inhibition of LOX-1 prevents inflammation and photoreceptor cell death in retinal degeneration. Int. Immunopharmacol., Vol. 80. 10.1016/j.intimp.2020.106190.